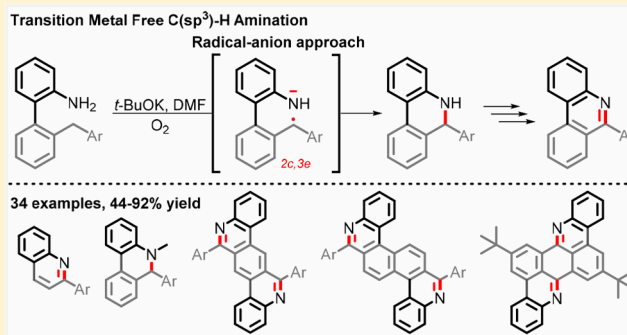


Coupling N–H Deprotonation, C–H Activation, and Oxidation:
Metal-Free C(sp³)–H Aminations with Unprotected AnilinesChristopher J. Evoniuk,[†] Gabriel dos Passos Gomes,[†] Sean P. Hill,[†] Satoshi Fujita,[‡]
Kenneth Hanson,[†] and Igor V. Alabugin^{*,†}[†]Florida State University, Tallahassee, Florida 32306, United States[‡]Interdisciplinary Graduate School of Engineering Sciences, Kyushu University, Fukuoka, Fukuoka Prefecture 819-0395, Japan

Supporting Information

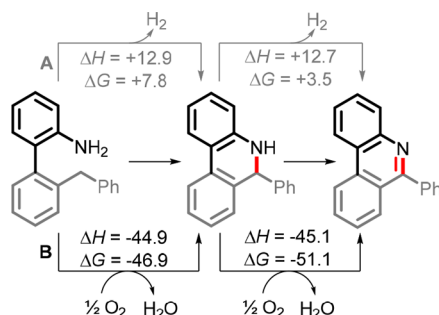
ABSTRACT: An intramolecular oxidative C(sp³)–H amination from unprotected anilines and C(sp³)–H bonds readily occurs under mild conditions using *t*-BuOK, molecular oxygen and *N,N*-dimethylformamide (DMF). Success of this process, which requires mildly acidic N–H bonds and an activated C(sp³)–H bond (BDE < 85 kcal/mol), stems from synergy between basic, radical, and oxidizing species working together to promote a coordinated sequence of deprotonation: H atom transfer and oxidation that forges a new C–N bond. This process is applicable for the synthesis of a wide variety of *N*-heterocycles, ranging from small molecules to extended aromatics without the need for transition metals or strong oxidants. Computational results reveal the mechanistic details and energy landscape for the sequence of individual steps that comprise this reaction cascade. The importance of base in this process stems from the much greater acidity of transition state and product for the 2c,3e C–N bond formation relative to the reactant. In this scenario, selective deprotonation provides the driving force for the process.



INTRODUCTION

Direct construction of a C–N bond from a C(sp³)–H bond and an N–H bond is a challenging transformation in organic chemistry,¹ especially, when an unprotected primary amine is used as a partner for the notoriously unreactive C–H bonds.² Even with the large amount of work conducted in this area, only a few literature methods for C(sp³)–H amination do not rely on transition metals (TMs). This is not surprising because a typical $\text{RNH}_2 + \text{R}_2\text{CH}_2 \rightarrow \text{RN}=\text{CR}_2$ conversion of unprotected amines³ to an imine with the loss of two H₂ molecules is thermodynamically unfavorable ($\Delta G = +11$ kcal/mol, Scheme 1, path A).

Scheme 1. Thermodynamics of C–N Bond Formations from C–H/N–H Partners^a



^aA: dehydrogenative; B: oxidative.

The first N–C bond formation in this sequence is uphill by 8 kcal/mol (Scheme 1, top left). Even though C–H/N–H coupling becomes thermodynamically favorable when coupled with oxidation ($\Delta G = -47$ kcal/mol, Scheme 1, path B), significant kinetic barriers for the individual steps associated with the breaking of strong N–H and C–H bonds continue to provide challenges in the design of a practical version of this reaction.

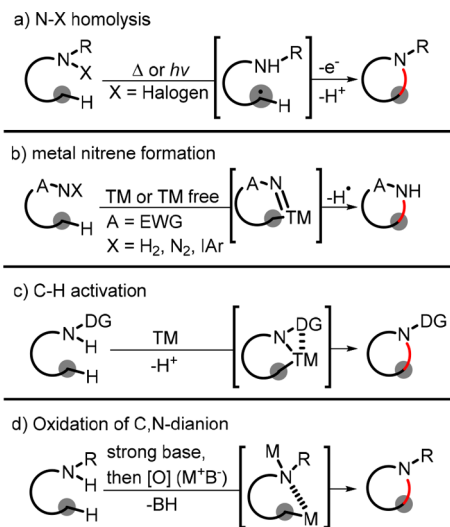
Early advances in C(sp³)–H amination chemistry go back to the Hoffman–Löffler–Freitag (HLF) reaction that utilized homolysis of the nitrogen–halogen bonds to form a nitrogen centered radical that performs hydrogen atom transfer (HAT) to afford cyclic amination products after oxidation and proton transfer (Scheme 2a).⁴ More recently, C–H activation was accomplished through the insertion of metal nitrenoids into C–H bonds (Scheme 2b).⁵ The power of transition metals can be controlled and amplified by appropriately designed directing groups (DGs) that assist with the formal metal insertion into the C–H bond, that is finally oxidized by an intramolecular amino group (Scheme 2c).⁶

We have recently reported a FeCl₃-mediated oxidative approach to C–H amination with anilines based on a sequence of electron and proton transfers.⁷ Although this approach is conceptually appealing, we reasoned that if SET is coupled to

Received: July 19, 2017

Published: October 16, 2017

Scheme 2. Selected Approaches to C–H Amination



anionic conditions then milder oxidants can be used. An important step toward realizing this type of reactivity was earlier demonstrated by Sarpong and co-workers who involved a C,N dianion into a C–N bond-forming reaction by a mild in situ oxidation (Scheme 2d).⁸

A conceptually simple approach that can couple N–H and C–H activation without the need to form a highly reactive dianion involves a sequence of N–H deprotonation and H-abstraction at an activated C–H bond,⁹ followed by an oxidation of the intermediate radical anion. The final step would convert a 2c,3e “half-bond” formed in the first two steps into a “normal” 2c,2e N–C bond. After the covalent C–N bond is formed, the above sequence of steps can be repeated to yield a C=N unit as the product of a double N–H/C–H activation (Scheme 3).

Although conceptual simplicity of this approach is appealing, finding the right combination of oxidant, radical, and base that can work together is a daunting task, especially for unprotected amine reagents susceptible to oxidation. We report the successful C(sp³)–H amination/iminination cascades with unprotected amines (Scheme 3) based on the combination of potassium *tert*-butoxide (*t*-BuOK), molecular oxygen, and DMF. Comprehensive computational analysis reveals the unusual mechanistic

features of this tightly choreographed sequence of transformations. In the final part, we illustrate the synthetic power of this method via preparation of new families of *N*-heterocyclic polyaromatic π -acceptors.

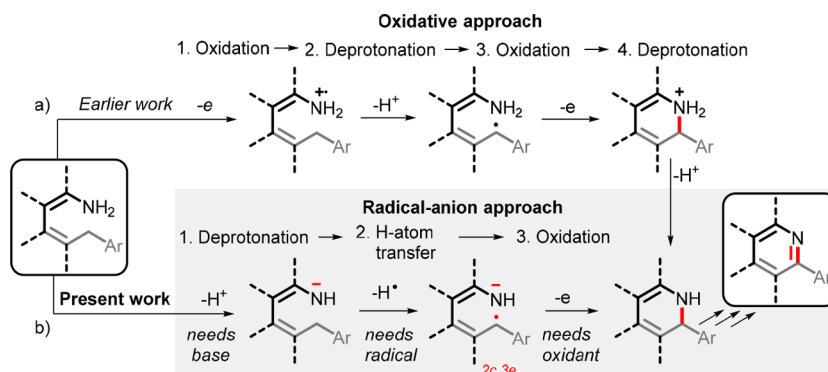
RESULTS

Following the general synthesis route outlined in the Supporting Information, we prepared model substrate **1a** (full details in Supporting Information) that has the prerequisite of a mildly acidic N–H bond¹⁰ and a weakened C(sp³)–H bond.^{11–13} We reacted **1a** (0.01 mmol) with *t*-BuOK (3-equiv) in acetonitrile (Table 1, entry 1) under air at reflux. Under these conditions, C–H amination product **2a** was not observed and starting material was reclaimed. Similarly, no reaction occurred in toluene (entry 2). However, when the reaction was performed in DMSO, product **2a** was observed in 18% yield with low conversion of the starting material (entry 3). Ultimately, full conversion was observed, and CH₂/NH₂ cross-coupling product **2a** was obtained in 78% yield when DMF was used as the solvent (entry 4). These results prompted us to carry out the remaining optimization studies in DMF. We then tested eight other bases (entries 5–12). Only the stronger alkoxide bases provided **2a** in good yields and conversion rates, with the *tert*-butoxide salts providing the best results (K, Na, and Li). The highest yields and conversions were observed using *t*-BuOK as the base. We also varied the equivalents of base used in the reaction (entries 15–17) and found the best results by using 3 equiv.


The role of an oxidant is illustrated by the much lower reactivity under the argon atmosphere (15% yield of **2a**, entry 13). In contrast, the use of O₂ as an oxidant improved conversion and yield in comparison to the standard atmospheric conditions (entry 14). Intriguingly, higher yields were observed at room temperature than at elevated temperatures for the model system (entries 18–20). The optimal conditions emerged from these experiments included the use of *t*-BuOK (3 equiv) under an O₂ atmosphere at room temperature in DMF in the presence of 4 Å molecular sieves (entry 20).

MECHANISTIC STUDIES

Several key experimental observations are listed below. First, deprotonation of ArNH₂ by *t*-BuOK is confirmed by deuterium exchange (Scheme 4, eq 1), with exclusive deuterium

Scheme 3. Comparison of the two approaches to making C=N moiety from the double activation of CH₂/NH₂ moieties^a

^a(a) Earlier reported oxidative approach: Oxidation of an aniline moiety increases C–H acidity in a stereoelectronically connected ArCH₂– group. Deprotonation can lead to the formation of a benzylic radical in the close proximity to the NH₂ group. Subsequent oxidation completes the first C–N bond formation. (b) New radical-anionic approach: N–H deprotonation weakens a remote C–H bond, setting the stage for radical C–H abstraction followed by the formation of a C–N bond. Once the C–N bond is formed, further C–H/N–H activation leads to the formation of a C=N bond bond, completing the formal imination of a CH₂ group.

Table 1. Optimization of Reaction Conditions^a


entry	base	atm	solvent	temp, °C	yields, % ^b	
					1a	2a
1	<i>t</i> -BuOK	air	MeCN	reflux	>99	<1
2	<i>t</i> -BuOK	air	MePh	90	>99	<1
3	<i>t</i> -BuOK	air	DMSO	90	53	18
4	<i>t</i> -BuOK	air	DMF	90	<1	78
5	Cs ₂ CO ₃	air	DMF	90	77	21
6	Na ₂ CO ₃	air	DMF	90	89	7
7	K ₂ CO ₃	air	DMF	90	85	14
8	CsF	air	DMF	90	65	18
9	NaOMe	air	DMF	90	29	48
10	KOMe	air	DMF	90	25	54
11	<i>t</i> -BuONa	air	DMF	90	18	62
12	<i>t</i> -BuOLi	air	DMF	90	39	42
13	<i>t</i> -BuOK	Ar	DMF	90	82	15
14	<i>t</i> -BuOK	O ₂	DMF	90	<1	83
15 ^c	<i>t</i> -BuOK	O ₂	DMF	90	53	38
16 ^d	<i>t</i> -BuOK	O ₂	DMF	90	44	54
17 ^e	<i>t</i> -BuOK	O ₂	DMF	90	<1	78
18	<i>t</i> -BuOK	O ₂	DMF	50	<1	83
19	<i>t</i> -BuOK	O ₂	DMF	rt	<1	88
20 ^f	<i>t</i> -BuOK	O ₂	DMF	rt	<1	88
21	none	O ₂	DMF	rt	>99	<1

^aReaction conditions: **1a** (0.01 mmol), base (3 equiv), solvent (0.5 mL) at specified temperature (rt = 23 °C) for 4 h. ^bDetermined by ¹H NMR using internal standard. ^cUsing 1 equiv of base. ^dUsing 2 equiv of base. ^eUsing 4 equiv of base. ^fMolecular sieves (4 Å) were used in reaction.

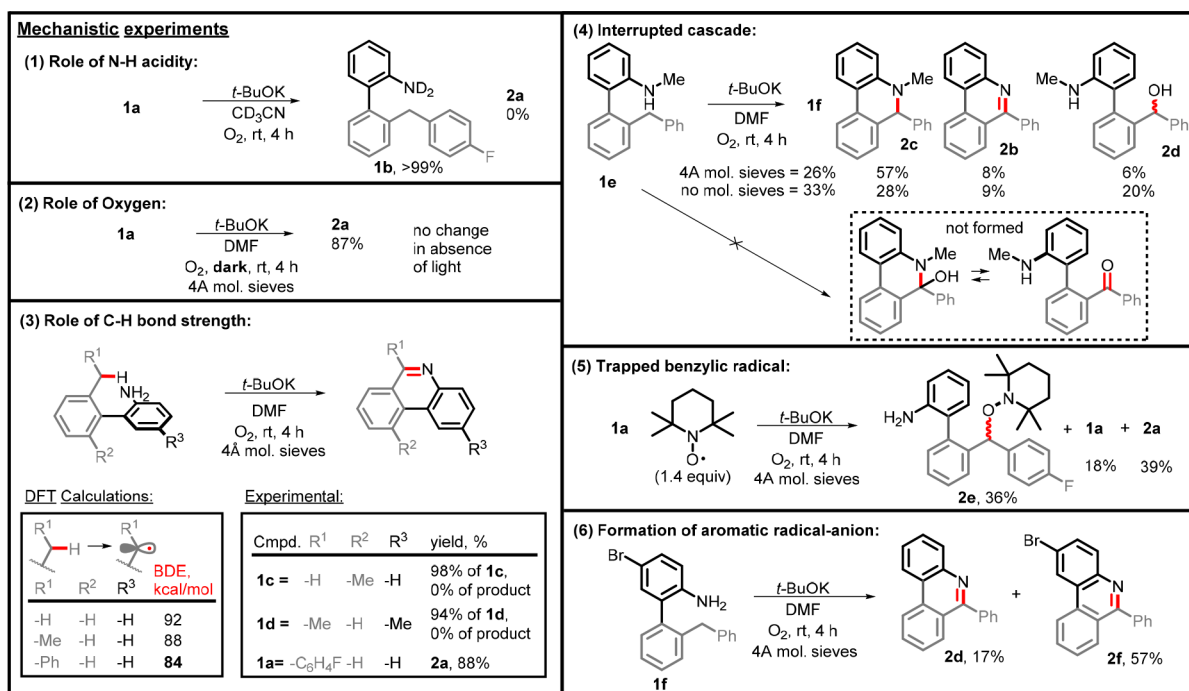
incorporation at the nitrogen position. Second, the reaction was conducted in the dark without any deleterious effects on the outcome (Scheme 4, eq 2). Third, the role of C–H bond strength was illustrated by the lack of reaction at the less activated benzylic C(sp³)–H bonds with Me- and Et-substituted biphenyls **1c** and **1d** under the optimized conditions (Scheme 4, eq 3). We have also calculated the bond dissociation energies (BDEs) of the benzylic C–H with similar substitution patterns to the compounds studied experimentally. The calculated BDE threshold for H-abstraction to occur under these conditions is in the vicinity of 85 kcal/mol.

On the basis of the recent reports of benzylic oxidations under similar conditions,¹⁴ one could suggest that the new reaction proceeds through oxidation of C(sp³)–H to form a carbonyl intermediate, followed by fast condensation with the anilide anion driven by aromatization via the loss of H₂O. To investigate the presence of a carbonyl intermediate, we used NH–Me analogue **1e** to successfully interrupt the reaction (Scheme 4, eq 4). The absence of oxygen-bearing functionalities in compound **2c** where only the single C–N bond is formed (Scheme 4, eq 4) provides evidence for the direct coupling of the C(sp³)–H and N–H groups.¹⁵

Since *N*-methylaniline readily undergoes demethylations under base-promoted homolytic aromatic substitution (BHAS) reactions, the latter reaction can proceed further and yield varying amount of fully aromatized product **2b**.¹⁶ We also observed that water is detrimental for reaching the full conversion with the more challenging substrates, as evidenced in byproduct **2d**. Because 2 equiv of water are formed for each mole of product, we found that the yields can be improved by adding 4 Å molecular sieves to the reaction mixture.

The formation of a stabilized radical at the benzylic position in the presence of DMF/*t*-BuOK¹⁷ was confirmed by successful trapping of this species with TEMPO, a common trapping reagent for free radicals (Scheme 4, eq 5).¹⁸ A Br-containing substrate, **1f**, was prepared to investigate the ability of these

Scheme 4. Selected Mechanistic Experiments



reagents to undergo SET, and under our conditions, **2f** was formed along with dehalogenated product **2d** in about a ~3:1 ratio (Scheme 4, eq 6). This observation supports an electron transfer mechanism with an aromatic radical anion as an intermediate that can either eject a halide anion or be intercepted in a different way (*vide infra*).^{17a,19}

The combination of the above observations suggests a base-mediated electron-transfer C–N coupling as a plausible pathway for this C–H amination (Scheme 3, bottom).²⁰ This pathway takes advantage of the N-anion and C-radical that were supported by the above experiments. The formation of benzylic radicals under these conditions is consistent with the detection of radical species in the reaction of DMF and DMSO with base in the earlier EPR studies.^{14,21} Furthermore, these species (likely DMF radicals) were used for generating benzylic radicals via hydrogen atom transfer (HAT) from weakened Ar–C(sp³)–H bonds.^{15,22} Recently, formation of carbamoyl radicals from *t*-BuOK in DMF under very mild conditions was suggested as a byproduct of coupling reactions of enols with such weak oxidants as aryl iodides through an electron-transfer mediated S_{RN}1 pathway.²³ In the following part of the manuscript, we will analyze the individual steps of this sequence of transformations first and discuss the overall energy landscape at the end.

COMPUTATIONAL DETAILS

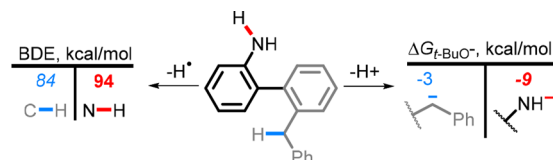
Guided by these experimental results, we turned to computations for charting the overall energy landscape and identifying the key intermediates of this chemical transformation. Thermodynamic calculations were carried using the meta-hybrid (U)M06-2X functional²⁴ and the 6-31+G(d,p) basis set for all atoms, with an ultrafine integration grid (99 590 points). A broken-spin approach was applied when necessary. The implicit SMD²⁵ solvation model was used to simulate the effects of *N,N*-dimethylformamide (DMF) throughout the calculated structures. Grimme's D3 version (zero damping) for empirical dispersion²⁶ was also included. Unless otherwise noted, all results presented are at the (SMD = DMF)/(U)M06-2X(D3)/6-31+G(d,p)/int = ufine level of theory. We opted for the hybrid PBE0 functional²⁷ to describe HOMO–LUMO gaps of the larger systems. Frequency calculations were carried for all structures to confirm them as either a minimum or a TS. We used nucleus-independent chemical shift (NICS)^{28,29} scans to evaluate local aromaticity in the polyaromatic systems. All calculations were performed with the Gaussian 09 software package.³⁰ Three-dimensional structures and orbital plots were produced with CYLView 1.0.1,³¹ IQmol 2.8.0,³² and Chemcraft 1.8.³³

DEPROTONATION/H ATOM TRANSFER

Calculations support *tert*-butoxide anion being sufficiently basic to deprotonate ArNH₂ and generate anilide anion in a downhill process ($\Delta G = -9$ kcal/mol). Although the *t*-BuO anion is predicted to be sufficiently basic to remove the proton from the benzylic Ar₂CH₂ group, formation of the N-centered anion is calculated to be more exergonic because of the greater acidity of the N–H bond, (9 vs 3 kcal, Scheme 5).

In contrast, the bis-benzylic C–H bond is more reactive toward homolytic cleavage than the aniline N–H bonds (the BDEs of 84 and 94 kcal/mol, respectively). The difference in the C–H and N–H BDEs suggest that H atom abstraction should proceed at the benzylic position and form a

Scheme 5. N–H Bonds Are Prone to Selective Deprotonation, Whereas C–H Bonds Are Prone to Selective H-Atom Transfer

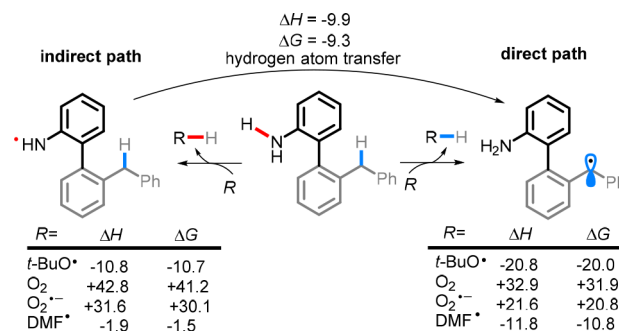


C-centered radical. Interestingly, the benzylic C–H BDE in the N-deprotonated species is slightly increased (85.5 kcal/mol). The lack of BDE lowering suggests that, in the twisted reactant, communication between the negative charge and the spin is unimportant and these two centers remain effectively distonic.⁹ Alternatively, the N-anion can be oxidized into an N-centered radical that can abstract the benzylic C–H intramolecularly.

We have considered molecular oxygen, superoxide, *t*-BuO radical, and C(O)NMe₂ radical derived from DMF as the key species that can serve as radicals and/or oxidizing agents (Scheme 7). Although molecular oxygen is the primary reactant, it cannot serve directly as efficient radical C–H activator. Calculations suggest that H atom abstraction becomes exergonic only with the more reactive *t*-BuO and C(O)NMe₂ radicals (Scheme 6).

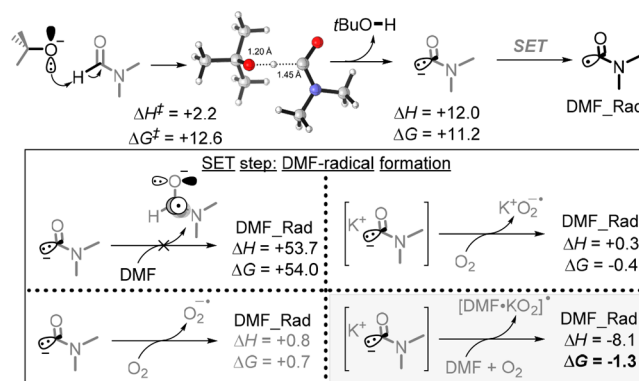
Given the reaction conditions, we suggest that C(O)NMe₂ radical derived from DMF is the key species that can perform H-abstraction at the Ar–CH₂–R position which produces

Scheme 6. Two Approaches to Benzylic C–H Activation^a



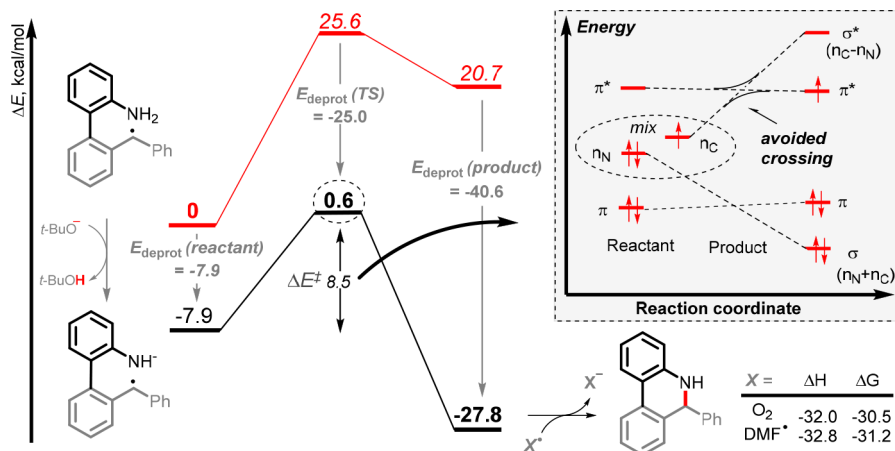
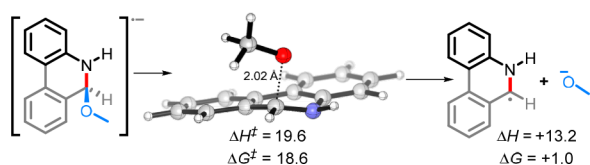
^aEnergies in kcal/mol.

Scheme 7. DMF Cannot Oxidize DMF Anion, whereas Oxygen Does so Favorably^a



^aEnergies in kcal/mol.

Scheme 8. Effect of Deprotonation on Kinetic and Thermodynamics of 2c,3e Bond Formation

Scheme 9. Elimination of MeO Anion from a Cyclic Radical Anion^a^aEnergies in kcal/mol.

radical anion in an exergonic step. Hence, the overall success of transformation would depend on finding a way for making these high energy reactive intermediates under the reaction conditions.

■ ROLE OF DMF RADICAL

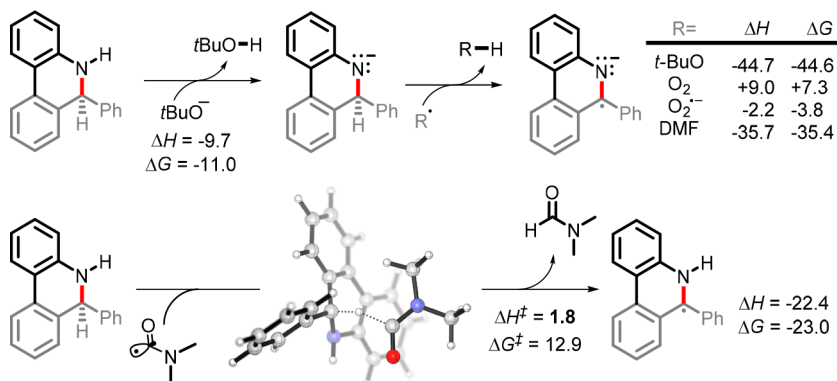
In this section, we discuss a difficult part of this cascade—the role of potassium *tert*-butoxide, DMF and oxygen in the formation of radicals needed to perform the C–H activation step of the cascade. The difficulty begins with the deprotonation of DMF by *tert*-butoxide. DMF is 9.5 pK_a units less acidic than *t*-BuOH in water (pK_a (DMF in H₂O) = 26.5,³⁴ pK_a (*t*-BuOH in H₂O) = 17). Hence, deprotonation of DMF by *t*-BuOK is thermodynamically uphill. DMF deprotonation reported by Reeves and co-workers used stronger bases than *t*-BuOK (*t*-BuLi or lithium diisopropylamide (LDA)).³⁵ Although we could not find the pK_a of DMF in DMF or DMSO in the literature (pK_a (*t*-BuOH in DMSO) = 29.4), according to

our calculations, deprotonation of DMF by *t*-BuO anion is ~11 kcal/mol endergonic in DMF. Even though thermodynamics of this process are unfavorable, a small amount of DMF anion is still formed at the equilibrium. Indeed, ¹H and ¹³C experiments conducted by Drapeau and co-workers verified the fast exchange of the formamide proton in a wet solution of DMF-*d*₇ with *t*-BuOK.²³

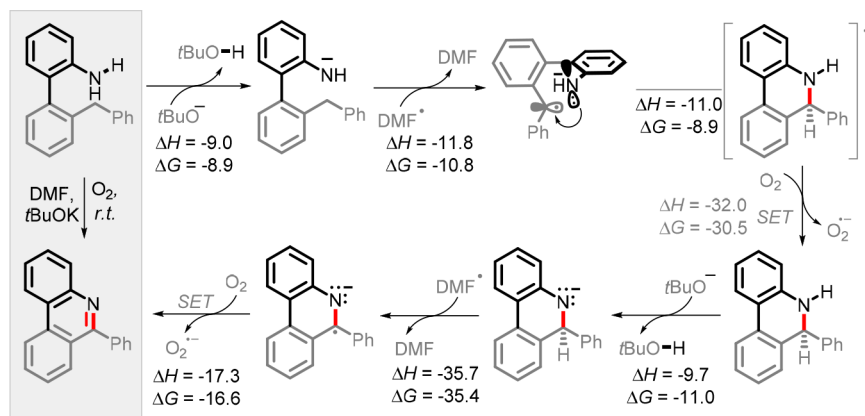
Drapeau and co-workers have shown computationally that the cation provides stabilization to the DMF anion formed following deprotonation.²³ They found that in the case of Li⁺ too much stabilization can be detrimental to the reaction cascade, essentially creating a potential energy well that the intermediates could not escape, whereas the stabilization provided by K⁺ was sufficient to establish reasonable reaction barriers for their reaction. Recent computational analysis by Houk and co-workers in a *t*-BuOK-mediated dehydrogenative C–H silylation reaction showcased the benefit of K⁺ over Na⁺ in key steps of their mechanism.³⁶ We have briefly explored the effects of cation on the anionic pathways outlined in this work and found that they do not change the main trends for most of the steps (see [Supporting Information](#) for additional details). Considering the above, we have only introduced K⁺ and DMF in our computational model for the “problematic” DMF radical formation step (*vide infra*).

Once the DMF anion is formed, our computations suggest that its oxidation with oxygen is close to thermoneutral. Inclusion of potassium counterion in the computational model makes this electron transfer slightly exergonic. Hence, the overall combination of deprotonation and oxidation is

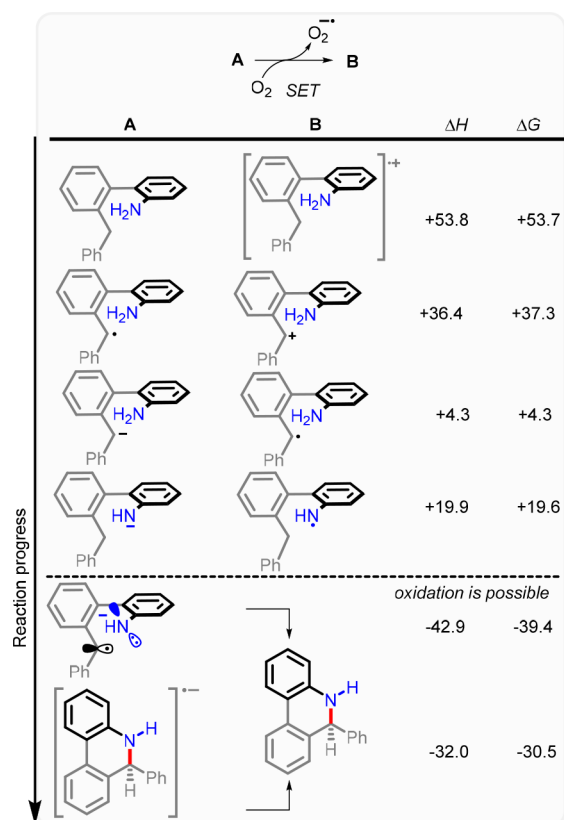
Scheme 10. Activation of the Non-Aromatic Product of the First Stage of the Cascade



Scheme 11. Thermodynamic Landscape for the Double C–H/N–H Amination Cascade



Scheme 12. Free Energies (kcal/mol) for Electron Transfer to Molecular Oxygen Illustrate the “Build-Up” of Reductive Potential along the Path of the Reaction



~10 kcal/mol uphill and thus should be capable of producing only very small concentrations of DMF radicals at the equilibrium.³⁷ However, this situation is not uncommon in autoxidation processes (for example, the notorious reaction of THF with oxygen) and can still lead to efficient transformations. In other words, as long as steps propagating the cascade are fast and efficient, the endergonicity of the initiation step simply corresponds to ~10 kcal/mol penalty needed for reaching the rate-limiting transition state for the overall cascade. However, oxidation of a DMF anion by another molecule of DMF with the formation of a DMF radical and a DMF radical anion, suggested earlier in the literature,^{17b,c} is highly energetically unfavorable.

2C,3E C–N BOND FORMATION/OXIDATION

Once the C,N radical anion is formed, its cyclization is exergonic due to the formation of a 2c,3e bond at the shorter N...C distances. The importance of the negative charge at this step is illustrated by the comparison of the evolution of 2c,3e interaction in the neutral amine and the deprotonated analogue. In the neutral system, the C–N bond formation is ~20 kcal/mol uphill, whereas it becomes >10 kcal/mol exergonic in the anionic case. One can suggest that destabilization of non-bonding electrons in the lone pair by the negative charge can serve as a source of increased reactivity. Furthermore, presence of the π -system in the cyclized product allows an additional way to stabilize the additional electron by “ejecting”³⁸ it from the three-electron C–N “half-bond” into the π^* -orbital. In other words, presence of an orthogonal π -system facilitates the C–N bond formation by preventing the extra electron from going to the very high energy $\sigma_{\text{C–N}}^*$ orbital (Scheme 8). Instead, such electron-transfer between the σ - and π -systems leads to formation of a normal 2c,2e N–C bond and a delocalized π -anion with a low activation barrier of ~8.9 kcal/mol in an overall downhill process (~12 kcal/mol).

Scheme 8 further illustrates that the advantage of radical anionic process over its neutral counterpart is in the much greater acidity of the cyclic TS for the 2c,3e C–N bond formation in comparison to the acyclic reactant state. Reaction acceleration by deprotonation may be a powerful general concept for the control of chemical reactivity (see Supporting Information for details on the influence of K^+ on this step).³⁹ The presence of K^+ increases the activation barrier for the cyclization step by ~4 kcal/mol, resulting in an unproductive effect on the overall reaction.

Importantly, the cyclic anion–radical readily transfers an electron to molecular oxygen with the formation of superoxide anion in a highly exergonic step ($\Delta G = -31$ kcal/mol) that finishes the first C–N bond formation. In this scenario, the C–H/N–H activation is accomplished via N–H deprotonation, C–H radical abstraction, and an electron transfer. Although electron transfer from the cyclic radical anion to the DMF radical is also potentially viable, it should be noted that oxygen should be more abundant under the reaction conditions where it can serve as a stoichiometric oxidant. In addition to “ejection” of electron via oxidation or MO crossing, the negative charge of radical–anion can also lead to anion elimination⁴⁰ as shown by facile loss of methoxide from the MeO substituted cyclized radical anion (Scheme 9).

■ SECOND CYCLE (FOR THE C=N BOND FORMATION)

Formation of the C=N bond can be initiated via two different pathways. In the first of them, deprotonation of the N–H bond or fast HAT to an external radical, such as the DMF-radical (Scheme 10). The subsequent highly exergonic HAT transfer is assisted via weakening of the C–H bond by the adjacent N-centered anion⁴¹ and strong stabilization of the formed radical via conjugation. In the radical anion, the C–H bond is so weak that even superoxide is capable of abstracting it in an exergonic fashion. Subsequent aromatization is promoted by oxidation to deliver the final product in a favorable step ($\Delta G = -16.6$ kcal/mol).

Alternatively, the benzylic C–H bond can be abstracted by a radical. This step can be fast and highly exergonic if DMF radical is used to perform HAT, to generate a relatively unreactive benzylic radical. However, it is reasonable to suggest that deprotonation of N–H is more likely given the concentration of *t*-BuO anion in the system when compared to the concentration of other radicals.

The overall cascade with the most relevant thermodynamic values is summarized in Scheme 11. The key C–N bond formation proceeds as a sequence of three mildly exergonic steps that is made irreversible by a highly exergonic electron transfer from the C,N radical-anion to oxygen.

An important feature of this transformation is the “build up” of reductive potential;⁴² the intermediate anions and radicals

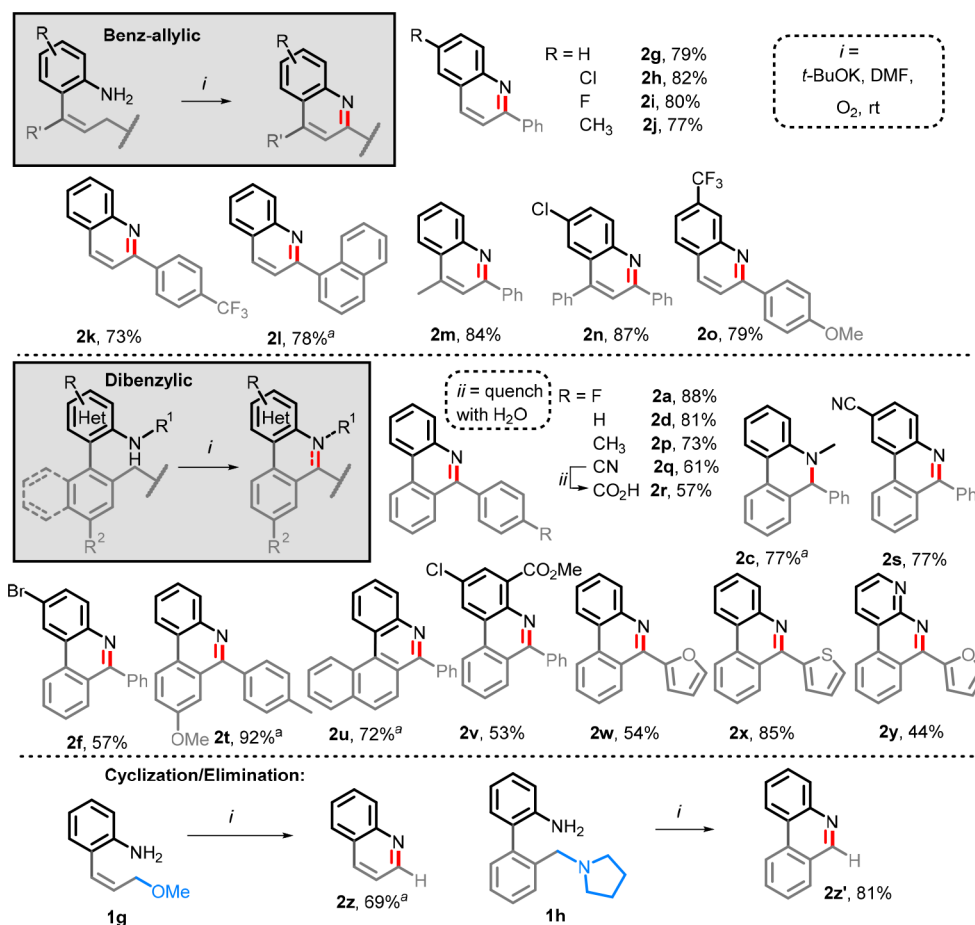
are weaker reductants in comparison to the radical-anions. Keeping the reductive potential low at the beginning prevents premature involvement of oxygen until we build a radical-anion that is easy to oxidize (Scheme 12). This oxidation can either directly provide the product (from the cyclic radical-anion) or lead to an open polar C,N diradicaloid species (from the acyclic radical-anion) that converge without barrier to the cyclic product *in silico*.^{43,44}

■ REACTION SCOPE

Benzylic C(sp³)–H bonds activated by a single π -system were insufficiently reactive under the reaction conditions (Scheme 4, eq 3) in mechanistic studies above. In contrast, doubly benzylic or “benz-allylic” CH₂ groups are readily involved in the C–N bond formation, suggesting the key role of radical H atom abstraction for the reaction success.

Electron-withdrawing (e.g., –CF₃, –CN, –CO₂Et, etc.) and moderately electron-donating groups (–CH₃) were well-tolerated. As an aside, an aqueous workup should be avoided with base sensitive functional groups to prevent hydrolysis (as evidenced by the conversion of –CN → –CO₂H, product 2q → 2r). However, strongly donating functional groups required longer reaction times and, occasionally, elevated temperature. Certain halogen substituents (–F, –Cl, and –CF₃) are also compatible with the reaction conditions. However, as mentioned earlier, Br-substituted substrate 1f underwent reductive debromination to a small degree, an observation

Scheme 13. Substrate Scope for Multiple Successful Approaches to Prepare a Diverse Library of N-Heterocycles^a

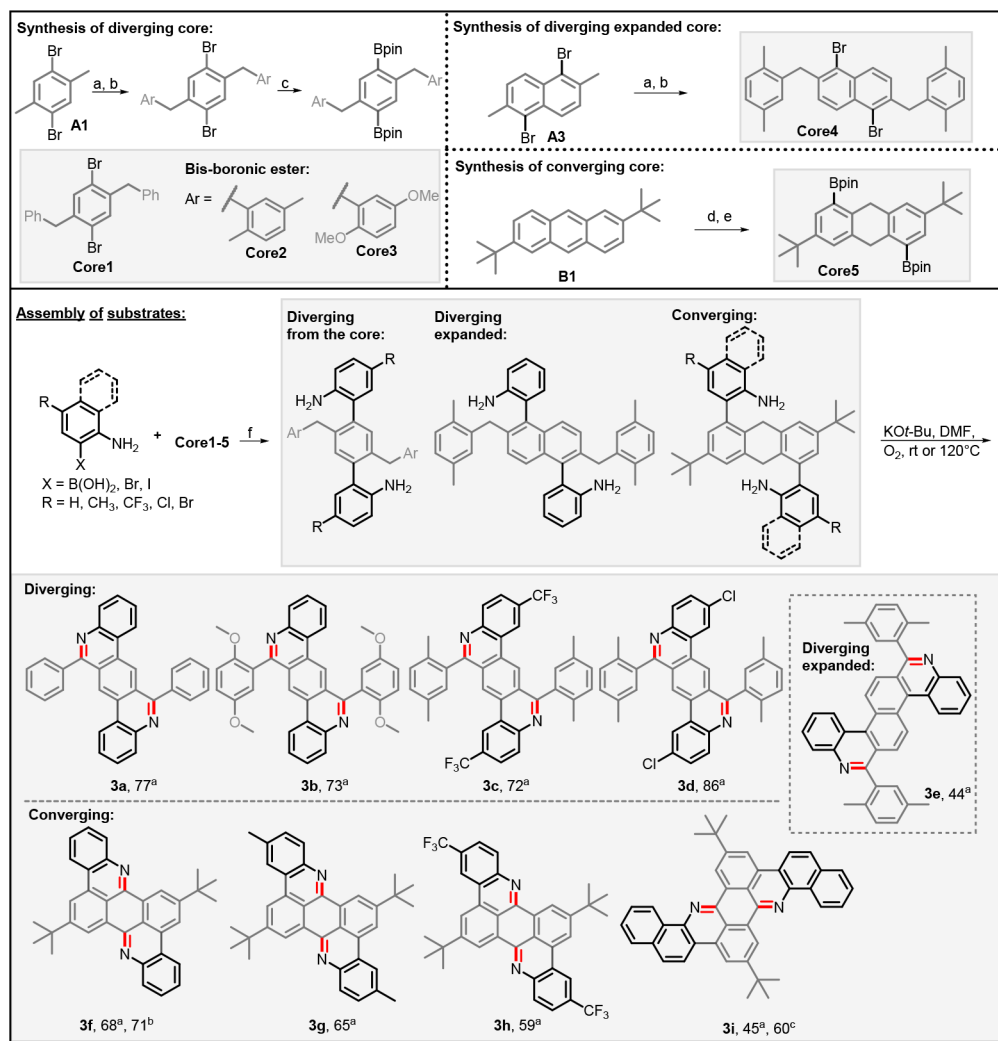


^aUnless otherwise stated, yields are of the isolated product. Yield determined by ¹HNMR.

that further supports an electron transfer mechanism. Additional substitution ($-\text{CH}_3$, $-\text{Ph}$) at the α -position of alkene

reactants has no deleterious effect on the yields of the corresponding products (**2m** and **2n**). Substrates containing

Scheme 14. Alternative Approaches That Allow Assembly of Three Different Heterocycle Families and List of Extended Polyaromatics Available through the Double CH_2/NH_2 Coupling Reactions^a



^aSynthesis of precursors and substrates for the cyclization of bis-structures **3a**–**i**. (a) NBS, BPO, C₆H₆, reflux. (b) AlCl₃, PhNO₂, Ar–H, 110°C. (c) Pd(dppf)Cl₂ • CH₂Cl₂, B₂pin₂, KOAc, DMSO. (d) Na, *t*-BuOH, THF, rt. (e) [Ir(COD)OMe₂], TMPhen (3,4,7,8-tetramethylphenanthroline), B₂pin₂, THF, 85°C. (f) Pd(PPh₃)₄, K₂CO₃, PhMe, EtOH, H₂O (5:2:1) reflux.

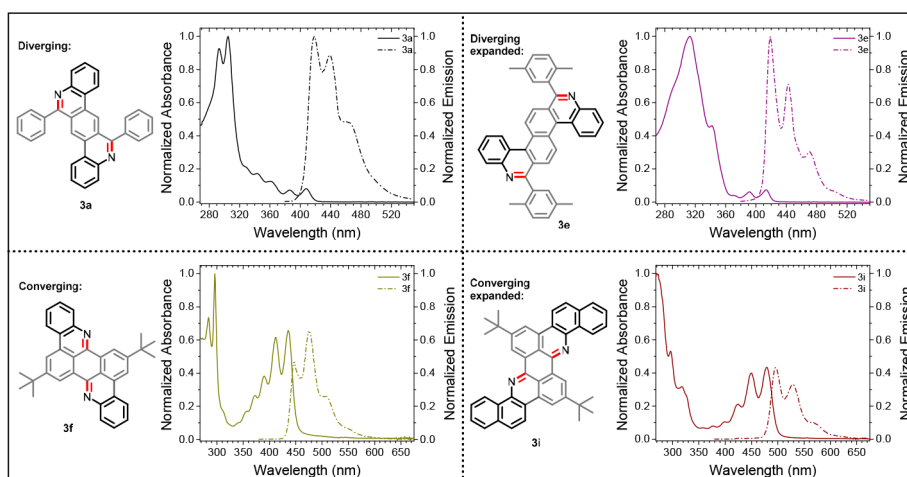


Figure 1. Absorption and emission spectra for structures **3a**, **3e**, **3f**, and **3i**. Please see the [Supporting Information](#) for full experimental details.

heterocyclic units, both on the aniline ring and at the C(sp³)-H terminus (**2w**, **2x**, and **2y**), readily participate in the double C-H/N-H activation as well.

The addition of a heteroatomic functionality to the benzylic/allylic group also weakens the C(sp³)-H bond and allows for C-N bond formation to occur. In the latter case, fragmentation of the benzyl/allyl heteroatom group takes place, which is in agreement with the proposed radical-anionic mechanism.⁴⁵ The second combination of cyclization and fragmentation expands the utility of this method to the preparation of unsubstituted *N*-heterocycles.

■ EXTENDED *N*-HETEROAROMATICS

The key step to assemble our C(sp³)-H amination precursors is a Suzuki coupling of a diborylated aromatic moiety with an

appropriate *o*-aminoaryl halide or the reverse approach that utilizes an aromatic dihalide and an *o*-amino boronic ester. The building blocks for the key step are available from dimethyl aromatics via a sequence of benzylic bromination followed by Friedel-Crafts alkylation using benzene and *p*-xylene as the aromatic nucleophile to prepare **Core1** and **Core4** respectively (Scheme 13). Additionally, 1,4-dimethoxybenzene and *p*-xylene were used as the aromatic nucleophiles prior to a Miyaura borylation to provide **Core2** and **Core3**, respectively (Scheme 13). Synthesis of diborylated dihydroanthracene core, **Core5** (Scheme 13), was accomplished using innovative chemistry recently reported by Zhang and co-workers.⁴⁶ The synthetic pathway is scalable with **Core2** and **Core5** being prepared on a gram scale (**Core2** = 1.3 g, **Core5** = 3 g, Scheme 13).

Expansion of this protocol to the preparation of extended aromatics demonstrates the far-reaching applications of this synthetic methodology. We prepared a variety of extended *N*-heterocyclic compounds by developing a modular simple synthesis that starts from the easily modified cores. Depending on whether the CH₂ groups are located at the opposite or adjacent positions of the pre-existing cycles, the ring annulation via bis-cascades can either diverge from or converge to the core of the structure. These cascades provide distinctly different heterocycles and illustrate the flexibility of our synthetic methodology.

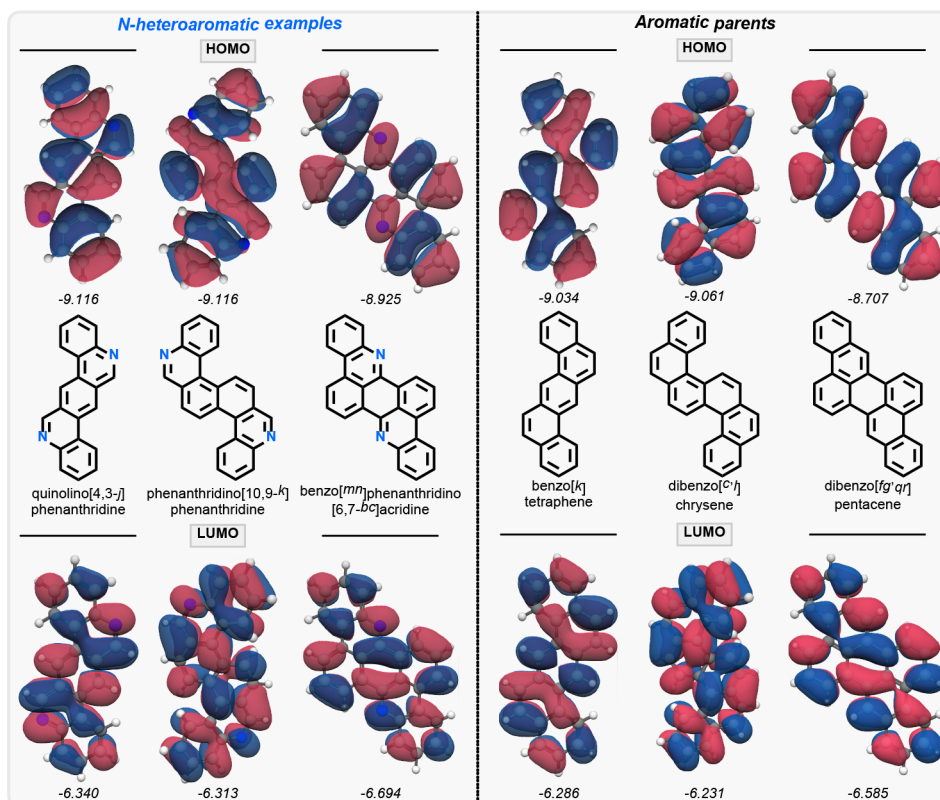
Gratifyingly, the bis-cascade reaction only required slight modification to the earlier optimized conditions and applied to assemble extended *N*-heterocyclic aromatics in a short synthesis pathway from commercially available anilines in moderate to good yields (Scheme 13). The diverging bis-substrates only

Table 2. Photophysical Data for Compounds 3a–i

compd	λ_{abs} (nm)	λ_{em} (nm) ^b	τ (ns) ^b	Φ ^c	$E_{0,0}$ (eV) ^d
3a	305, 408	418	2.9	0.13	3.00
3b	290, 404	418	5.1	0.04	3.04
3c	299, 400	406	1.7	0.28	3.06
3d	307, 401	406	1.1	0.08	3.05
3e	313, 413	418	4.1	0.07	2.97
3f	296, 437	475	2.3	0.49	2.81
3g	301, 442	485	2.5	0.57	2.74
3h	295, 435	473	2.2	0.81	2.80
3i	270, 479	489	2.7	0.39	2.50

^aUV and visible region peak values. ^bExcitation at 360 nm. ^cCalculated relative to DPA in chloroform at room temperature ($\Phi = 1.00$).⁴⁷ ^d $E_{0,0}$ calculated from crossover wavelength of absorption and emission spectra.

Scheme 15. Comparison of Structures and Frontier MOs for the *N*-Derivatives Prepared in This Work with Their Hydrocarbon Parents^a



^aHOMO and LUMO energies, at the PBE0(D3)/6-31+G(d,p) level of theory, are in eV.

required a slight modification to the equivalents of *t*-BuOK used in the reaction (6 instead of 3 equiv). In contrast, the converging bis-substrates required not only 6 equiv of *t*-BuOK but also elevated temperatures (120 °C instead of room temperature). Interestingly, when a bis-diverging substrate where R = Br was placed under the elevated temperatures, full cleavage of the Br substituent occurred to provide **3f**. In accordance with our earlier result in mechanistic studies, this finding further corroborates the formation of radical anion. With this short list of modifications, we successfully prepared new extended *N*-heteroaromatics with varying functionality (Scheme 14).

■ PHOTOPHYSICAL PROPERTIES

We investigated the electronic structure of all of the extended *N*-heterocycles by UV-vis absorption and fluorescence spectroscopy (Figure 1, Table 2). The divergent and convergent series of extended *N*-heterocycles, **3a–3i**, have two distinct absorption bands in the UV/vis spectra: one (λ_{max}) around 300 nm and another past 400 nm.

The lowest energy transition for **3a**, **3b**, **3c**, **3d**, and **3e** corresponds to a weak absorbance above 400 nm and is apparently partially forbidden. The difference between normal and extended cores for the diverging series does not lead to a large change in the absorbance energy (418 vs 418 nm for **3a** vs **3e**). The weak response to the increase in the size of the core may originate from the distorted geometry of **3e**, which corresponds to a fused bis-[4]helicene and, thus, is bent from planarity.⁴⁸ However, the converging series (**3f**, **3g**, **3h**, and **3i**) show strong hyperchromism for the absorbance above 400 nm. The absorbance for the lowest transition is presumably due to the differences in planarity and conjugation of the chromophoric units for each respective series and the transition probability of their dipole moment.

All of the extended *N*-heterocycles are fluorescent with emission above 400 nm. The observed trends follow a pattern similar to the absorption data, with the spectra for the convergent cores being bathochromically shifted about 60 nm relative to the divergent series. The quantum yields for the divergent series (**3a–3e**) are rather low ($\Phi = 4\text{--}13\%$, Table 2), with the exception of **3c** ($\Phi = 28\%$). Conversely, the quantum yields for the convergent series (**3f–3i**) are dramatically improved ($\Phi = 39\text{--}81\%$, Table 2).

■ ROLE OF N ATOMS IN ELECTRONIC PROPERTIES OF POLYAROMATICS

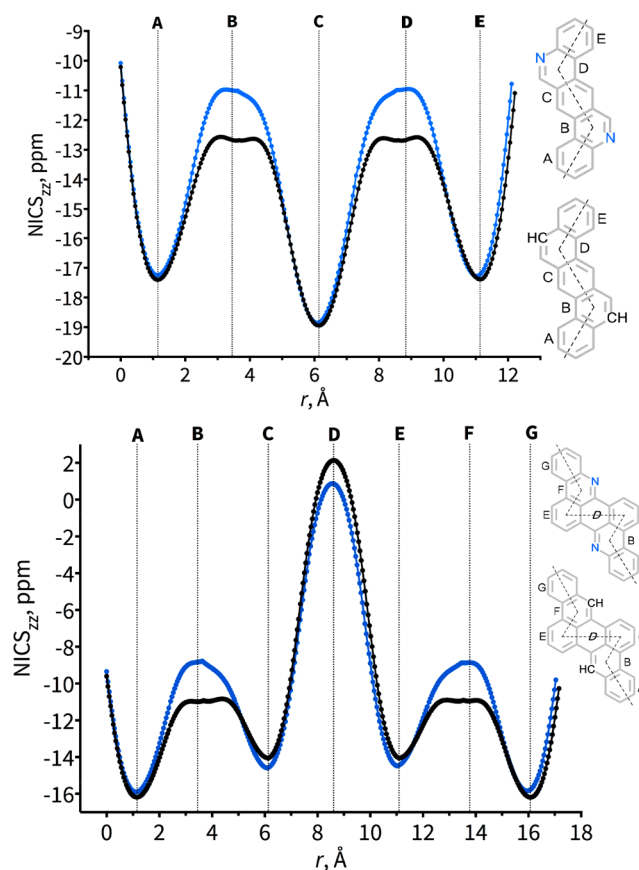
The new synthetic sequences outlined in this work provided concise routes to the *N*-heterocyclic analogues of benzo[*k*]-tetraphene, dibenzo[*c,l*]chrysene, and dibenzo[*fg,qr*]pentacene. The parent hydrocarbons have been reported in the past.⁴⁹ However, the literature reports lack complete sets of photophysical data. Due to scarcity of experimental information, we have calculated the frontier MOs and analyzed the effect of *N*-heteroatom incorporation on these orbitals.

Comparison of the HOMO and LUMO nodal structures for the *N*-heterocycles and their hydrocarbon parents illustrate that orbital symmetry is quite robust and not influenced strongly by the introduction of two nitrogen atoms. Only two of the six pairs of FMOs (the HOMOs of phenanthridino[10,9-*k*]phenanthridine and dibenzo[*c,l*]chrysene) are significantly different (Scheme 15). This observation is consistent with the general features observed in the electronic absorption spectra

for the new heterocycles. In agreement with the experimental data, TD-DFT analysis of the lowest energy excitations for the *N*-containing systems found that the first excited states for the “diverging” systems correspond to weakly allowed states with multiple contributors, of which the HOMO–LUMO transition is the major one. For the convergent ring system, the lowest excited state has a much larger oxidation state and corresponds almost entirely to a HOMO–LUMO transition.

The local aromaticity analysis via NICS-*xy* scans is able to detect noticeable differences in the electronic structures of these three pairs of carbo/heterocycles. For example, the two *N*-containing rings of quinolino[4,3-*j*]phenanthridine are less aromatic than the analogous rings of benzo[*k*]tetraphene (Scheme 16).⁵⁰

Scheme 16. Selected Changes in Local Aromaticity Revealed by the NICS-*xy* Scans



■ CONCLUSIONS

We have developed a direct method for converting C(sp³)-H and N-H bonds into C-N bonds in the presence of base, molecular oxygen, and DMF. Each reaction component plays a separate role in the synergistic effort which involves a coordinated sequence of deprotonation, H atom transfer, and electron transfer for each C-N bond formation. *t*-Butoxide base plays two roles: (a) It deprotonates nitrogen and (b) provides sufficient concentration of deprotonated DMF that can be converted into a DMF radical. The role of DMF radical is in selective activation of the C-H bond partner in C-N bond formation via HAT that forms a C-centered radical. The C-N bond is formed initially as a 2c,3e interaction between the *N*-anion and C-radical, a process that is assisted by state

crossing “ejecting” the extra electron into an orthogonal π -system and forging a “normal” $2c,2e$ C–N bond. This process of $2c,3e$ bond formation becomes much faster and more favorable thermodynamically when aniline is deprotonated, indicating that both the TS and the product of the “neutral” version of this process are considerably more acidic than the starting benzylic radical (Scheme 8). Oxidation of the cyclic radical–anion intermediate by molecular oxygen finishes the sequence of deprotonation, HAT, and oxidation that are necessary for the success of this deceptively simple transformation. The process opens a quick access to the previously unknown classes of extended N-heterocycles.

■ ASSOCIATED CONTENT

Supporting Information

The Supporting Information is available free of charge on the ACS Publications website at DOI: 10.1021/jacs.7b07519.

Full experimental details, ^1H NMR, ^{13}C NMR, HR-MS, and NMR spectra for all newly reported compounds. UV–vis and emission spectra along all photophysical data are available for extended N-heteroaromatics, and computational details for all calculated structures (PDF)

■ AUTHOR INFORMATION

Corresponding Author

*alabugin@chem.fsu.edu

ORCID

Christopher J. Evoniuk: 0000-0002-9595-4004

Gabriel dos Passos Gomes: 0000-0002-8235-5969

Kenneth Hanson: 0000-0001-7219-7808

Igor V. Alabugin: 0000-0001-9289-3819

Notes

The authors declare no competing financial interest.

■ ACKNOWLEDGMENTS

The fundamental and synthetic aspects of this study were supported by donors of the ACS Petroleum Research Fund (PRF#57377-ND4) and by the National Science Foundation (CHE-1465142). We appreciate the allocation of computational resources from FSU RCC and the NSF XSEDE (TG-CHE160006). F.S. is grateful for support from An Educational and Research Promotion (Overseas Scientific Activity) Program 2016 for Doctor Course Students, Interdisciplinary Graduate School of Engineering Sciences, Kyushu University, and Prof. M. Shindo.

■ REFERENCES

- (1) (a) Park, Y.; Kim, Y.; Chang, S. *Chem. Rev.* **2017**, *117*, 9247. (b) Louillat, M.-L.; Patureau, F. W. *Chem. Soc. Rev.* **2014**, *43*, 901. (c) Collet, F.; Lescot, C.; Dauban, P. *Chem. Soc. Rev.* **2011**, *40*, 1926. (d) Jeffrey, J. L.; Sarpong, R. *Chem. Sci.* **2013**, *4*, 4092. (e) Collet, F.; Dodd, R. H.; Dauban, P. *Chem. Commun.* **2009**, *34*, 5061. (f) Thansandote, P.; Lautens, M. *Chem. - Eur. J.* **2009**, *15*, 5874. (g) Wang, X.; Xia, D.; Qin, W.; Zhou, R.; Zhou, X.; Zhou, Q.; Liu, W.; Dai, X.; Wang, H.; Wang, S.; Tan, L.; Zhang, D.; Song, H.; Liu, X.-Y.; Qin, Y. *Chem.* **2017**, *2*, 803.
- (2) (a) Zatolochyna, O. V.; Gevorgyan, V. *Nat. Chem.* **2014**, *6*, 661. (b) Jun, C.-H.; Lee, J. H. *Pure Appl. Chem.* **2004**, *76*, 577. (c) Shi, Z.; Larock, R. C. *Top. Curr. Chem.* **2009**, *292*, 123.
- (3) Example of synthetic advantages of unprotected amines: Nguyen, K. M. H.; Langeron, M. *Eur. J. Org. Chem.* **2016**, *2016*, 1025.
- (4) (a) Hofmann, A. W. *Ber. Dtsch. Chem. Ges.* **1883**, *16*, 558. (b) Löffler, K.; Freytag, C. *Ber. Dtsch. Chem. Ges.* **1909**, *42*, 3427.

(c) Wolff, M. E. *Chem. Rev.* **1963**, *63*, 55. (d) Chen, K.; Richter, J. M.; Baran, P. S. *J. Am. Chem. Soc.* **2008**, *130*, 7247.

(5) (a) Breslow, R.; Gellman, S. H. *J. Am. Chem. Soc.* **1983**, *105*, 6728. (b) Intrieri, D.; Mariani, M.; Caselli, A.; Ragaini, F.; Gallo, E. *Chem. - Eur. J.* **2012**, *18*, 10487. (c) Roizen, J. L.; Harvey, M. E.; Du Bois, J. *Acc. Chem. Res.* **2012**, *45*, 911. (d) Davies, H. M. L.; Manning, J. R. *Nature* **2008**, *451*, 417. For an elegant “metalloradical catalysis” approach to C–H amination, see: (e) Lu, H.-J.; Lang, K.; Jiang, H.-L.; Wojtas, L.; Zhang, X. P. *Chem. Sci.* **2016**, *7*, 6934. (f) Goswami, M.; Lyaskovskyy, V.; Domingos, S. R.; Buma, W. J.; Woutersen, S.; Troeppner, O.; Ivanovic-Burmazovic, I.; Lu, H.-J.; Cui, X.; Zhang, X. P.; Reijerse, E. J.; DeBeer, S.; van Schooneveld, M. M.; Pfaff, F.; Ray, K.; de Bruin, B. *J. Am. Chem. Soc.* **2015**, *137*, 5468. (g) Lu, H.-J.; Li, C.-Q.; Jiang, H.-L.; Lizardi, C. L.; Zhang, X. P. *Angew. Chem. Int. Ed.* **2014**, *53*, 7028.

(6) (a) Wasa, M.; Yu, J.-Q. *J. Am. Chem. Soc.* **2008**, *130*, 14058. (b) Rice, G. T.; White, M. C. *J. Am. Chem. Soc.* **2009**, *131*, 11707. (c) Yang, M.; Su, B.; Wang, Y.; Chen, K.; Jiang, X.; Zhang, Y.-F.; Zhang, X.-S.; Chen, G.; Cheng, Y.; Cao, Z.; Guo, Q.-Y.; Wang, L.; Shi, Z.-J. *Nat. Commun.* **2014**, *5*, 4707.

(7) Evoniuk, C. J.; Hill, S. P.; Hanson, K.; Alabugin, I. V. *Chem. Commun.* **2016**, *52*, 7138.

(8) (a) Bisai, A.; West, S. P.; Sarpong, R. *J. Am. Chem. Soc.* **2008**, *130*, 7222. (b) Gruver, J. M.; West, S. P.; Collum, D. B.; Sarpong, R. *J. Am. Chem. Soc.* **2010**, *132*, 13212. (c) Jeffrey, J. L.; Bartlett, E. S.; Sarpong, R. *Angew. Chem., Int. Ed.* **2013**, *52*, 2194.

(9) For large effects of remote anionic centers on radical stability, see (a) Gryn'ova, G.; Marshall, D. L.; Blanksby, S. J.; Coote, M. L. *Nat. Chem.* **2013**, *5*, 474. (b) Gryn'ova, G.; Coote, M. L. *J. Am. Chem. Soc.* **2013**, *135*, 15392. (c) Franchi, P.; Mezzina, E.; Lucarini, M. *J. Am. Chem. Soc.* **2014**, *136*, 1250. (d) Morris, M.; Chan, B.; Radom, L. *J. Phys. Chem. A* **2012**, *116*, 12381. (e) Morris, M.; Chan, B.; Radom, L. *J. Phys. Chem. A* **2014**, *118*, 2810.

(10) Use of N-centered reactive intermediates for C–N bond formation without C–H activation: (a) Wang, X.; Xia, D.; Qin, W.; Zhou, R.; Zhou, X.; Zhou, Q.; Liu, W.; Dai, X.; Wang, H.; Wang, S.; Tan, L.; Zhang, D.; Song, H.; Liu, X.-Y.; Qin, Y. *Chem.* **2017**, *2*, 803. Alabugin, I. V.; Harris, T. *Chem.* **2017**, *2*, 753. (b) Choi, G. J.; Knowles, R. R. *J. Am. Chem. Soc.* **2015**, *137*, 9226. (c) Romero, N. A.; Margrey, K. A.; Tay, N. E.; Nicewicz, D. A. *Science* **2015**, *349*, 1326. (i) Nguyen, T. M.; Manohar, N.; Nicewicz, D. A. *Angew. Chem., Int. Ed.* **2014**, *53*, 6198.

(11) (a) Bordwell, F. G.; Zhang, X. M.; Cheng, J. P. *J. Org. Chem.* **1993**, *58*, 6410. (b) Yu, A.; Liu, Y.; Li, Z.; Cheng, J.-P. *J. Phys. Chem. A* **2007**, *111*, 9978.

(12) Van Hoomissen, D. J.; Vyas, S. *J. Org. Chem.* **2017**, *82*, 5731.

(13) Brandi, P.; Galli, C.; Gentili, P. *J. Phys. Org. Chem.* **2006**, *19*, 552.

(14) Wang, H.; Wang, Z.; Huang, H.; Tan, J.; Xu, K. *Org. Lett.* **2016**, *18*, 5680.

(15) Zhu, X.-Q.; Li, X.-T.; Han, S.-H.; Mei, L.-R. *J. Org. Chem.* **2012**, *77*, 4774.

(16) Yang, H.; Zhang, L.; Jiao, L. *Chem. - Eur. J.* **2017**, *23*, 65.

(17) (a) Barham, J. P.; Coulthard, G.; Emery, K. J.; Doni, E.; Cumine, F.; Nocera, G.; John, M. P.; Berlouis, L. E. A.; McGuire, T.; Tuttle, T.; Murphy, J. A. *J. Am. Chem. Soc.* **2016**, *138*, 7402. (b) Wang, W.; Zhao, X.; Tong, L.; Chen, J.; Zhang, X.; Yan, M. *J. Org. Chem.* **2014**, *79*, 8557. (c) Chen, Y.; Zhang, X.; Yuan, H.; Wei, W.; Yan, M. *Chem. Commun.* **2013**, *49*, 10974. (d) Chen, J.; Chen, Z.; Zhao, H.; Zhang, T.; Wang, W.; Zou, Y.; Zhang, X.; Yan, M. *Org. Biomol. Chem.* **2016**, *14*, 4071.

(18) TEMPO product was identified by ^1H NMR and HR-MS.

(19) (a) Emery, K. J.; Murphy, J. A.; Tuttle, T. *Org. Biomol. Chem.* **2017**, *15*, 920. (b) Barham, J. P.; Coulthard, G.; Kane, R. G.; Delgado, N.; John, M. P.; Murphy, J. A. *Angew. Chem., Int. Ed.* **2016**, *55*, 4492.

(20) Studer, A.; Curran, D. P. *Nat. Chem.* **2014**, *6*, 765.

(21) Øpstad, C. L.; Melo, T.-B.; Sliwka, H.-R.; Partali, V. *Tetrahedron* **2009**, *65*, 7616.

(22) Chen, Y.; Zhang, N.; Ye, L.; Chen, J.; Sun, X.; Zhang, X.; Yan, M. *RSC Adv.* **2015**, *5*, 48046.

- (23) Pichette Drapeau, M.; Fabre, I.; Grimaud, L.; Ciofini, I.; Ollevier, T.; Taillefer, M. *Angew. Chem., Int. Ed.* **2015**, *54*, 10587.
- (24) The M06-2X functional has demonstrated good thermodynamic data for organic reactions. For more details, see (a) Zhao, Y.; Truhlar, D. G. *Theor. Chem. Acc.* **2008**, *120*, 215. (b) Zhao, Y.; Truhlar, D. G. *Acc. Chem. Res.* **2008**, *41*, 157.
- (25) Marenich, A. V.; Cramer, C. J.; Truhlar, D. G. *J. Phys. Chem. B* **2009**, *113*, 6378.
- (26) Grimme, S.; Antony, J.; Ehrlich, S.; Krieg, H. *J. Chem. Phys.* **2010**, *132*, 154104.
- (27) Adamo, C.; Barone, V. *J. Chem. Phys.* **1999**, *110*, 6158.
- (28) Chen, Z.; Wannere, C. S.; Corminboeuf, C.; Puchta, R.; Schleyer, P. v. R. *Chem. Rev.* **2005**, *105*, 3842.
- (29) NICS-xy scans were performed at the (GIAO)B3LYP/6-311+G* level of theory, with ultrafine grid for integral and fine grid for CPHF. The step distance was 0.05 Å. We used Prof. Amnon Stanger's Aroma for the NICS-scans calculations. For full details, see (a) Rahalkar, A.; Stanger, A. *Aroma*; <http://chemistry.technion.ac.il/members/amnon-stanger/>. (b) Stanger, A. *J. Org. Chem.* **2006**, *71*, 883. (c) Stanger, A. *J. Org. Chem.* **2010**, *75*, 2281. (d) Gershoni-Portan, R.; Stanger, A. *Chem. - Eur. J.* **2014**, *20*, 5673.
- (30) Frisch, M. J.; Trucks, G. W.; Schlegel, H. B.; Scuseria, G. E.; Robb, M. A.; Cheeseman, J. R.; Scalmani, G.; Barone, V.; Mennucci, B.; Petersson, G. A.; Nakatsuji, H.; Caricato, M.; Li, X.; Hratchian, H. P.; Izmaylov, A. F.; Bloino, J.; Zheng, G.; Sonnenberg, J. L.; Hada, M.; Ehara, M.; Toyota, K.; Fukuda, R.; Hasegawa, J.; Ishida, M.; Nakajima, T.; Honda, Y.; Kitao, O.; Nakai, H.; Vreven, T.; Montgomery, J. A., Jr.; Peralta, J. E.; Ogliaro, F.; Bearpark, M.; Heyd, J. J.; Brothers, E.; Kudin, K. N.; Staroverov, V. N.; Kobayashi, R.; Normand, J.; Raghavachari, K.; Rendell, A.; Burant, J. C.; Iyengar, S. S.; Tomasi, J.; Cossi, M.; Rega, N.; Millam, J. M.; Klene, M.; Knox, J. E.; Cross, J. B.; Bakken, V.; Adamo, C.; Jaramillo, J.; Gomperts, R.; Stratmann, R. E.; Yazyev, O.; Austin, A. J.; Cammi, R.; Pomelli, C.; Ochterski, J. W.; Martin, R. L.; Morokuma, K.; Zakrzewski, V. G.; Voth, G. A.; Salvador, P.; Dannenberg, J. J.; Dapprich, S.; Daniels, A. D.; Farkas, O.; Foresman, J. B.; Ortiz, J. V.; Cioslowski, J.; Fox, D. J. *Gaussian 09*, revision E.01; Gaussian, Inc.: Wallingford, CT, 2009.
- (31) Legault, C. Y. *CYLview*, 1.0b; Université de Sherbrooke: Sherbrooke, Quebec, Canada, 2009 (<http://www.cylview.org>).
- (32) *IQmol*, 2.8.0, 2017. <http://iqmol.org>.
- (33) *ChemCraft*, 1.8. <http://www.chemcraftprog.com> (accessed February 2016).
- (34) Heumann, W. R.; Bouchard, A.; Tremblay, G. *Can. J. Chem.* **1967**, *45*, 3129.
- (35) Reeves, J. T.; Tan, Z.; Herbage, M. A.; Han, Z. S.; Marsini, M. A.; Li, Z.; Li, G.; Xu, Y.; Fandrick, K. R.; Gonnella, N. C.; Campbell, S.; Ma, S.; Grinberg, N.; Lee, H.; Lu, B. Z.; Senanayake, C. H. *J. Am. Chem. Soc.* **2013**, *135*, 5565.
- (36) (a) Liu, W.-B.; Schuman, D. P.; Yang, Y.-F.; Toutov, A. A.; Liang, Y.; Klare, H. F. T.; Nesnas, N.; Oestreich, M.; Blackmond, D. G.; Virgil, S. C.; Banerjee, S.; Zare, R. N.; Grubbs, R. H.; Houk, K. N.; Stoltz, B. M. *J. Am. Chem. Soc.* **2017**, *139*, 6867. (b) Banerjee, S.; Yang, Y.-F.; Jenkins, I. D.; Liang, Y.; Toutov, A. A.; Liu, W.-B.; Schuman, D. P.; Grubbs, R. H.; Stoltz, B. M.; Krenske, E. H.; Houk, K. N.; Zare, R. N. *J. Am. Chem. Soc.* **2017**, *139*, 6880.
- (37) Furthermore, recombination of the DMF and superoxide radicals is highly thermodynamically favorable ($\Delta G = -47.6$ kcal/mol) and can provide an additional deactivation pathway for the DMF radical.
- (38) Peterson, P.; Shevchenko, N.; Breiner, B.; Manoharan, M.; Lufti, F.; Delaune, J.; Kingsley, M.; Kovnir, K.; Alabugin, I. V. *J. Am. Chem. Soc.* **2016**, *138*, 15617.
- (39) (a) Dewanji, A.; Mück-Lichtenfeld, C.; Studer, A. *Angew. Chem., Int. Ed.* **2016**, *55*, 6749. (b) Jeffrey, J. L.; Terrett, J. A.; MacMillan, D. W. C. *Science* **2015**, *349*, 1532.
- (40) (a) Doni, E.; O'Sullivan, S.; Murphy, J. A. *Angew. Chem., Int. Ed.* **2013**, *52*, 2239. (b) Ankner, T.; Hilmersson, G. *Tetrahedron* **2009**, *65*, 10856. (c) Papin, C.; Doisneau, G.; Beau, J.-M. *Chem. - Eur. J.* **2009**, *15*, 53.
- (41) For the large facilitating effect of anionic centers at the homolytic scission of adjacent bonds, see (a) Pal, R.; Clark, R. J.; Manoharan, M.; Alabugin, I. V. *J. Org. Chem.* **2010**, *75*, 8689. (b) Menon, A. S.; Bally, T.; Radom, L. *J. Phys. Chem. A* **2012**, *116*, 10203.
- (42) For the "upconversion" of reductants in chemical reactions, see Syroeshkin, M. A.; Krylov, I. B.; Hughes, A. M.; Alabugin, I. V.; Nasybullina, D. V.; Sharipov, M. Yu.; Gulyai, V. P.; Terent'ev, A. O. *J. Phys. Org. Chem.* **2017**, *30*, e3744.
- (43) It is also beneficial, of course, that oxidation of the acyclic intermediates can still provide the same overall products as discussed above. For example, an intramolecular H-atom transfer to the N-radical can give benzylic C-radical that can be deprotonated to return the reaction back on the radical-anionic path.
- (44) For related work on super electron donors, see (a) Murphy, J. A. *J. Org. Chem.* **2014**, *79*, 3731. (b) Zhou, S.; Anderson, G. M.; Mondal, B.; Doni, E.; Ironmonger, V.; Kranz, M.; Tuttle, T.; Murphy, J. A. *Chem. Science* **2014**, *5*, 476.
- (45) (a) Baciocchi, E.; Del Giacco, T.; Lanzalunga, O.; Lapi, A. *J. Org. Chem.* **2007**, *72*, 9582. (b) Baciocchi, E.; Del Giacco, T.; Lapi, A. *Org. Lett.* **2004**, *6*, 4791. (c) Haddach, A. A.; Kelleman, A.; Deaton-Rewolinski, M. V. *Tetrahedron Lett.* **2002**, *43*, 399. (d) Hauser, A.; Bohlmann, R. *Synlett* **2016**, *27*, 1870.
- (46) Zhang, G.; Rominger, F.; Zschieschang, U.; Klauk, H.; Mastalerz, M. *Chem. - Eur. J.* **2016**, *22*, 14840.
- (47) Bowen, E. J.; Sahu, J. *J. Phys. Chem.* **1959**, *63*, 4.
- (48) Selected references pertaining to helicenes: (a) Mohamed, R. K.; Mondal, S.; Guerrero, J. V.; Eaton, T. M.; Albrecht-Schmitt, T. E.; Shatruk, M.; Alabugin, I. V. *Angew. Chem., Int. Ed.* **2016**, *55*, 12054. (b) Mori, K.; Murase, T.; Fujita, M. *Angew. Chem., Int. Ed.* **2015**, *54*, 6847. (c) Upadhyay, G. M.; Talele, H. R.; Bedekar, A. V. *J. Org. Chem.* **2016**, *81*, 7751. (d) Lovinger, A. J.; Nuckolls, C.; Katz, T. J. *J. Am. Chem. Soc.* **1998**, *120*, 264. (e) Fujikawa, T.; Segawa, Y.; Itami, K. *J. Am. Chem. Soc.* **2015**, *137*, 7763. (f) Waghay, D.; Bagdziunas, G.; Jacobs, J.; Van Meervelt, L.; Grazulevicius, J. V.; Dehaen, W. *Chem. - Eur. J.* **2015**, *21*, 18791. (g) Hosokawa, T.; Takahashi, Y.; Matsushima, T.; Watanabe, S.; Kikkawa, S.; Azumaya, I.; Tsurusaki, A.; Kamikawa, K. *J. Am. Chem. Soc.* 2017 DOI: [10.1021/jacs.7b07113](https://doi.org/10.1021/jacs.7b07113)
- (49) (a) Umeda, R.; Miyake, S.; Nishiyama, Y. *Chem. Lett.* **2012**, *41*, 215. (b) Takahashi, I.; Hayashi, M.; Fujita, T.; Ichikawa, J. *Chem. Lett.* **2017**, *46*, 392. (c) Badger, G. M.; Donnelly, J. K.; Spotswood, T. M. *Aust. J. Chem.* **1964**, *17*, 1138. (d) Caronna, T.; Gabbadini, S.; Mele, A.; Recupero, F. *Helv. Chim. Acta* **2002**, *85*, 1. (e) Braude, E. A.; Fawcett, J. S. *J. Chem. Soc.* **1951**, *0*, 3113.
- (50) For the dramatic effects of N-substitution on the electronic properties of polyaromatics, see (a) Tverskoy, O.; Rominger, F.; Peters, A.; Himmel, H.-J.; Bunz, U. H. F. *Angew. Chem., Int. Ed.* **2011**, *50*, 3557. (b) Bunz, U. H. F.; Engelhart, J. U.; Lindner, B. D.; Schaffroth, M. *Angew. Chem., Int. Ed.* **2013**, *52*, 3810. (c) Bunz, U. H. F. *Chem. - Eur. J.* **2009**, *15*, 6780. (d) Fogel, Y.; Kastler, M.; Wang, Z.; Andrienko, D.; Bodwell, G. J.; Müllen, K. *J. Am. Chem. Soc.* **2007**, *129*, 11743. (e) Wang, Z.; Gu, P.; Liu, G.; Yao, H.; Wu, Y.; Li, Y.; Rakesh, G.; Zhu, J.; Fu, H.; Zhang, Q. *Chem. Commun.* **2017**, *53*, 7772. (f) Endres, A. H.; Schaffroth, M.; Paulus, F.; Reiss, H.; Wadepohl, H.; Rominger, F.; Krämer, R.; Bunz, U. H. F. *J. Am. Chem. Soc.* **2016**, *138*, 1792. (g) Gu, P.-Y.; Wang, Z.; Liu, G.; Yao, H.; Wang, Z.; Li, Y.; Zhu, J.; Li, S.; Zhang, Q. *Chem. Mater.* **2017**, *29*, 4172.